NASA Technical Memorandum 89906

# Finite Element Analysis of Flexible, Rotating Blades



Oliver G. McGee
*Lewis Research Center*
*Cleveland, Ohio*

July 1987

NASA

# FINITE ELEMENT ANALYSIS OF FLEXIBLE, ROTATING BLADES

Oliver G. McGee*
National Aeronautics and Space Administration
Lewis Research Center
Cleveland, Ohio 44135



## SUMMARY

This report should be used as a reference guide when using the finite element method to approximate the static and dynamic behavior of flexible, rotating blades. Important parameters such as twist, sweep, camber, co-planar shell elements, centrifugal loads, and inertia properties are studied. Comparisons are made between NASTRAN elements through published benchmark tests. The main purpose of this report is to summarize blade modeling strategies and to document capabilities and limitations (for flexible, rotating blades) of various NASTRAN elements.

## INTRODUCTION

Rotating blades constitute vital components in several practical machines such as, turbofan and turboprop engines and helicopter rotors. They can feature variable cross sections and spanwise variations of sweep and pretwist. Because of their complex geometry, the finite element technique is a natural choice for structural dynamic analysis.

Until the mid-1960's, most of the structural dynamic analyses were based on continuum beam methods such as Rayleigh-Ritz, Myklestad, extended Holzer and Galerkin (see sample works of Rao and Carnegie (refs. 1 and 2)). In these methods the blade is idealized as a pretwisted cantilever beam. Hence, they are mainly useful for high aspect ratio blades. With increased geometric complexities of modern blades, finite element methods have become more commonplace for static and dynamic analyses. One widely used general purpose finite element program is NASTRAN.

To employ finite element methods for rotating blades, analysts have to use extra care to obtain reliable results. Specifically, this involves an investigation into element selection, grid modeling techniques, boundary conditions and effects of rotation. The purpose of this manual is to discuss applications of the finite element technique to rotating blade structures. Typical test problems are examined and solution procedures are reviewed and presented. Emphasis is directed towards NASTRAN.

## BACKGROUND

The finite element technique offers many options for the structural dynamic analysis of swept and twisted blades. It is common practice to use plate or shell elements of rectangular or triangular shapes. For vibration analysis of skewed cantilever plates, an early application of this technique

---

*Summary Faculty Fellow. Present address: Ohio State University, Columbus, Ohio 43210.

was used by Dawe (ref. 3) and Anderson, Irons and Zienkiewicz (ref. 4), using rectangular and triangular elements, respectively. Olson and Lindberg (ref. 5) employed the same technique for finding free vibration characteristics of highly cambered blades using rectangular cylindrical shell elements. Rawtani and Dokainish (refs. 6 and 7) reported static bending and free vibration results of twisted cantilever plates.

Presently, a joint government/industry/university research effort is being conducted to compare finite element methods for twisted cantilevered plates to experimental data. The study involves two phases: Phase I considers only non-rotating, twisted plates (refs. 10 to 12) and Phase II extends this effort for rotating plates (presently under investigation). What has evolved from the first phase of this study is that a wide variation in submitted finite element analyses exists and a careful application of this method is needed to accurately predict the vibratory characteristics of highly twisted cantilever plates.

Many of the finite element results reported in references 10 to 12 show mark disagreements in predicted natural frequencies, particularly for highly twisted plates. The triangular plate finite elements (including COSMIC/NASTRAN CTRIA2 models) were typically deficient as were half of the shell and three-dimensional solid element formulations. Models using SAP quadrilateral plates and MSC/NASTRAN CQUAD4 shells, showed good convergence over a wide range of geometric parameters.

Improved multiblade propeller engines, called propfans, are being developed. Unlike conventional propellers, propfan blades are thin, flexible, shell-like structures with variable sweep and twist along their span. They are subjected to relatively high rotational speeds that can cause large deformations at the blade tip. Because of the complex geometry of propfan blades, finite element methods are a natural choice for deformation analysis. However, recently documented finite element analyses of propfan blades have shown significant disagreements with experimental data of modal frequencies (ref. 13).

This report is the first of two that deals with the finite element analysis of flexible blade structures. A second report (refs. 44) is a primer that summarizes the use of NASTRAN's large displacement and normal mode analyses for flexible, rotating blades. In the present report, previously published static and dynamic benchmark test problems are documented as they relate to blade configuration parameters such as twist, sweep and camber. The report is organized as follows. A discussion is first given of the types of approximations likely to exist in a finite element analysis of practical blades. For completeness, applicable COSMIC and MSC/NASTRAN plate/shell and solid elements are briefly described. Additional topics related to the subject are examined, which include element comparisons, mesh arrangement and refinement, co-planar shell elements, inertia properties, and centrifugal forces. Numerical solutions and graphical comparisons, as reported by various investigators, are given.

## FINITE ELEMENT APPROXIMATIONS OF BLADE STRUCTURES IN NASTRAN

The structural analysis of flexible, rotating blades has evolved from simple beam theories to sophisticated finite element techniques. Finite element grids for these blades can be divided into two categories, two-dimensional and three dimensional. A two-dimensional finite element mesh links grid points on the blade's mid-surface by connecting these points with either flat plate or shell elements. A three-dimensional mesh involves more than one surface of grid points, with two or more nodes in the thickness direction. The grid points are connected with "solid" or "brick" elements.

A finite element analysis of rotating, arbitrarily-shaped blades using plates/shells or solids introduces four different types of approximations, as quoted from Clough and Wilson of reference 14.

"First is the geometric approximation involved in replacing the actual continuous structural surface by an assemblage of discrete structural elements" (ref. 14). For modeling of swept and twisted blade surfaces in NASTRAN, several structural elements are available in the form of flat triangles (TRIA2, TRIA3,TRIA6), flat rectangles (QUAD2,QUAD4,QUAD8) or hexahedrons (HEX8,HEX20, HEXA8,HEXA20). Each of these elements possess their own special features that are pertinent to rotating blade structural analysis (refs. 8 and 9).

"The second basic assumption is that the strains (and/or displacements) in each element may be only of limited form, as specified by a set of nodal interpolation (or "shape") functions" (ref. 14). Depending on the actual stress variation placed on the blade at a given rotational speed, these assumed displacement orders may provide a reasonably good approximation. The NASTRAN higher order elements (TRIA6,QUAD8,HEXA20,HEX32) that have quadratic or cubic displacement variations, may provide better results than the lower order elements for a given degree of mesh refinement. On the other hand, more refined elements that feature higher order displacement fields with additional global degrees of freedom (DOF) would not be suited for the format of NASTRAN's general element. A practical "rule of thumb" to consider in the analysis is that "simplest can be best." That is, theoretically, any inherent error found in the calculated results of a coarse mesh consisting of simpler finite elements tends to vanish as the mesh is refined.

"A third approximation which may be present in some finite element analyses is that the assumed displacement patterns may not maintain interelement compatibility as the blade structure is loaded and deformed" (ref. 14). It is quite apparent that the problem of "co-planar elements" arises when using NASTRAN's TRIA and QUAD shell elements in a large displacement analysis (NASTRAN SOLUTION 64 -- SOL64). This element breakdown comes from a variety of sources. For instance, when modeling blades with high sweep and/or twist, the chord dimension at sections along the span are such that many elements may have to be used to achieve a satisfactory level of solution accuracy. Element incompatibility can develop when neighboring elements meet at a finite angle during any particular iteration of SOL64. This causes the analysis to abort at the global level, because the shell elements have 5 local degrees of freedom (DOF) per node and the global transformation equations utilize 6 global DOF per node.

Finally, the fourth approximation is that the three-dimensional blade surface may be treated as a two-dimensional surface with simplifying constraints

on displacement variations through the blade thickness. In COSMIC/NASTRAN's TRIA2 and QUAD2 element formulations, the Kirchoff thin plate theory of plane sections is assumed. However, less restrictive assumptions of forming a shell element as a degenerate three-dimensional solid element can be advantageous. What results is that shear distortions may be accounted for without difficulty by this approach. Ahmad (ref. 16) used this approach by introducing a constraint that lines through the element thickness displace in translation or rotation without distortion. Zienkiewicz (ref. 15), Iron (ref. 16), and Pawsey (ref. 17) also used degenerate solid elements to analyze arbitrary thin shells. By using modified integration points to calculate shear strain energy terms in the solid elements, overly-stiff element behavior in bending was suppressed.

From a practical standpoint, a good finite element is not necessarily the one which exhibits a monotonic convergence. A more important criterion is that the deviation from the exact result should be small, even when the blade is subdivided in a relatively coarse mesh. This point is especially important when using more refined shell and solid element assemblages, since they require a great deal more computer memory and cost.

## DESCRIPTION OF NASTRAN'S PLATE/SHELL AND SOLID ELEMENTS

From the preceding discussion, it is apparent that the type of element utilized may have an effect on solution accuracy and rate of convergence. For completeness, this section presents, as a brief catalog, those NASTRAN plate/shell and solid elements that may be used. The elements are shown in figures 1 to 10. Their principal features are listed below.

COSMIC/NASTRAN plate elements have two uncoupled stress systems, i.e., membrane and bending. COSMIC/NASTRAN solid elements are based on a standard isoparametric formulation, where identical approximation functions are used for the element geometry and displacement. Differential stiffness formulations are used for both the plate and solid elements in COSMIC/NASTRAN. These elements are described below:

TRIA2 is a constant thickness triangular element with both in-plane and bending stiffness (fig. 1). The stiffness formulation is a superposition of a constant strain membrane triangle with linear displacement order and of a basic bending triangle with an eight term, cubic normal displacement order. Important details of the stiffness derivation include: (1) bending slopes of the element are obtained from the definition of transverse shear strain (assumed constant in the element), and (2) a constraint such that the bending slope about the x-axis varies linearly from side a-b (fig. 1). Two TRIA2 elements joined along this boundary will have continuous displacements and slopes at all points. Both lumped and consistent mass formulations can be used.

QUAD2 is a quadrilateral element comprised of two sets of overlapping triangular elements (fig. 2). The a-b sides of the basic NASTRAN triangle lies along a diagonal to ensure displacement and slope continuity within the element. Since membrane and bending stiffness coupling is not available in COSMIC/NASTRAN, the QUAD2 is formed by adding the effects of the overlapping quadrilateral membrane element (QDMEM) with those of the overlapping quadrilateral bending element (QDPLT).

OTHER PLATE/SHELL ELEMENTS Alternative element formulations based on previous analyses posted in the literature can be used in COSMIC/NASTRAN. For example, one might consider using the Clough bending triangle (ref. 18), which can be superimposed with a NASTRAN membrane triangle to form a flat shell element (fig. 3). However, this element is archaic for thin, flexible blade applications in that it imposes additional constraints to ensure displacement continuity within the element. Consistent mass formulations of this element produce vibration frequencies on the high side, because constraint approximations, used in the stiffness calculation, are progressively applied in the mass formulation.

A second choice might be COSMIC/NASTRAN's TRSHL element. This element is a higher order triangular shallow shell element. The element approximation comprises a quadratic membrane and a quintic normal displacement function. Usage of TRSHL is low, most likely as a result of its inferior convergence on shell benchmark test problems.

There is a more attractive alternative to using QUAD2 elements in COSMIC/NASTRAN. Because of its potential for modeling curved surfaces, a quadrilateral shell element can be formed (manually in NASTRAN) out of four subdomain triangles with corner nodes not in the same plane (see fig. 4). The a-b side of the basic NASTRAN triangle is placed on an exterior edge to ensure interelement continuity. The interior point c is located at the intersection of straight lines connecting the midpoints of the sides (or at the average of the four corner node coordinates). The membrane and bending DOF at point c can be condensed out of the stiffness equations. Thus, the quadrilateral effectively has only 20 DOF per element. Although static condensation of the interior node introduces an additional constraint on this element, its level of engineering accuracy is quite good. Similar elements proposed by Clough and Felippa (ref. 19) and Clough and Johnson (ref. 20) were placed in the SAP general purpose finite element program. The twisted plate results shown in reference 10 using these elements were shown to perform well against those of other finite element formulations.

HEX8 and HEX20 are standard eight and twenty noded isoparametric brick elements (figs. 5 and 6). The element geometry and displacements are approximated by linear and quadratic functions, respectively in the three local directions. The element coordinate systems are defined on the CHEXA Bulk Data cards. Material reference is specified on the PHEX card. Reduced order integration is available (via NGP-field on PHEX Bulk Data card) for both HEX8 and HEX20.

The MSC/NASTRAN element library includes both flat and curved shell elements, which support both membrane and bending action. The analyst has a choice of four control options (via MID fields on PSHELL card) for stiffness formulation: (1) membrane-only behavior, (2) bending-only behavior, (3) combined bending and membrane behavior, and (4) materially coupled membrane-bending behavior. These stiffness control parameters are important options for structural analyses. The shell elements in MSC/NASTRAN include the following:

TRIA3 and QUAD4 are the three noded triangular and the four noded quadrilateral elements, shown in figure 7 and 8, respectively. General capabilities include: (1) identical approximating functions for element geometry and displacements, (2) 5 DOF per node, i.e., two membrane displacements and one bending displacement and two bending rotations, (3) thickness can vary over the

element surface, (4) lumped and consistent mass formulation, (5) selective integration for shear terms (QUAD4 only), (6) enforcement of bending curvature compatibility (QUAD4 only), (7) transverse shear flexibility to account for bending behavior (QUAD4 only), and (8) full geometric nonlinearity. All forces and moments are evaluated at the centroid of the element. Use of QUAD4 elements requires that all interior angles be less than 180°. A special feature of the QUAD4 elements is that all points do not have to lie in one plane. When modeling highly swept and twisted blades, enough QUAD4 elements should be used so that individual element warping is small. According to (ref. 9), "for modeling curved shell structures a tentative rule is that the included angle per element should be 10° or less to obtain errors of 4 percent or less in deflections.

MSC/NASTRAN's curved shell elements are the following:

TRIA6 and QUAD8 are the six noded triangular and eight noded quadrilateral curved thin shell elements, respectively shown in figure 9 and 10. The assumed displacement and geometry of these elements are of higher-order than their low-order cousins, described above. Also, these curved shell elements can connect six and eight grid points, respectively and they contain all of the features of their flat shell counterparts. Note that QUAD8 uses a standard isoparametric formulation (i.e., identical approximation functions are used for both element geometry and displacements). QUAD8 does not have transverse shear flexibility terms like its QUAD4 counterpart. For the TRIA6 and QUAD8 elements, all forces and moments are evaluated at the centroid and at the vertices of the element.

MSC/NASTRAN's solid elements are the following:

HEXA8 and HEXA20 The HEXA series of elements (figs. 5 and 6) in MSC/NASTRAN are improvements to the HEX8 and HEX20 six-sided brick elements in COSMIC/NASTRAN. These elements use isoparametric representation to characterize the element behavior. The HEXA8 is the three-dimensional analogy of the two-dimensional bilinear quadratic QUAD4 element and the HEX20 is the three-dimensional extension of the two-dimensional biquadratic cubic QUAD8 element. The HEX8 element contains the same type of shear correction used to improve the membrane shear behavior of its two-dimensional cousin. In addition, a reduced order of integration (via IN-field on PSOLID card) can be used for the shear strain contributions to the stiffness calculations. This is discussed in the next section.

## STATIC AND DYNAMIC BENCHMARK TESTS FOR BLADE STRUCTURES

The proceeding element descriptions are insufficient to make a decision on which elements are best to use for a particular blade. Lacking in the NASTRAN documentation are the performance of its elements in standard benchmark test that are applicable to swept, twisted or cambered blades. For example, some test problems that measure efficiency of plate/shell or solid elements include: (1) Scordelis-Lo shell problem, (2) patch test (which measures convergence of an assemblage of elements), (3) untwisted cantilever beam with point load at the free end, (4) swept cantilever beam with point load at the free end, (5) swept plate with uniform load, (6) twisted cantilever beam with point load at the free end, (7) twisted cantilever plate (normal mode vibrations), and (8) cantilever blade with camber (normal mode vibrations). Many of

these tests have been documented in surveys of finite element codes, namely Fong and Jones (ref. 21) and Harder (ref. 22).

Although the results of these published tests do not completely test the elements, they are sufficient for making preliminary decisions regarding finite element modeling of practical blades. More importantly, they reveal inherent deficiencies in a number of the NASTRAN plate/shell and solid element formulations. The succeeding subsections examine these benchmark test problems. Specific blade modeling aspects are discussed such as irregularity of mesh arrangement, mesh refinement, element length and thickness ratios, element warp and skewness, and modified integration within elements.

## The Scordelis-Lo Shell

Figure 11 shows the problem and table I and figure 12 display the convergence behavior of NASTRAN QUAD and HEXA elements in a rather severe test of bending behavior. The data has been compiled from references 21 and 22. Figure 12 shows excellent convergence of QUAD4 between the analytical shallow shell and the exact deep shell solutions. This suggests that this element is quite suitable for highly cambered blade models. Although the results of TRIA2 tend to overshoot the mark, the convergence is inconclusive. With a coarse mesh this is to be expected, since the transverse shear strain is assumed constant in the TRIA2 element formulation. QUAD2 are typically overstiff even for large numbers of DOF. Transverse shear flexibility in QUAD4 explains its obvious suitability for this benchmark test problem.

To shed light on NASTRAN's higher order elements, consider the normalized vertical deflection data for the Scordelis-Lo shell in table I. This data reveals that QUAD4 and HEX8 exhibit a strong convergence from above, and that QUAD8 and reduced integration forms of HEX20 show an oscillatory pattern of convergence. Clearly, QUAD8 portrays the best numerical behavior for this problem with its quadratic shape functions for its geometry and displacements. QUAD2 and HEX20 (without reduced integration) are typically overstiff.

## The Patch Test

In some displacement-based element theories approximating functions may violate interelement continuity of displacements. This causes infinite strains along the element boundaries. Elements characterized by this behavior are called "nonconforming elements." In the limit the formulation may converge to the correct answer with increasing mesh refinement. Necessary conditions are (1) that zero strain exists in the element during rigid body motion and (2) that the assumed displacement function contains terms for which constant strain modes are obtained.

To ensure that convergence may be achieved, nonconforming elements must pass a patch test (ref. 40). This test involves an arbitrary assemblage of oddly shaped elements subjected to a constant strain/stress condition. If the resulting nodal displacements cause a constant stress state within the element, then the patch test is not violated. Nonconforming elements that pass this test have convergent results with mesh refinement, and at times will exhibit

better behavior than conforming elements. However, note that nonconforming elements that violate the patch test will not necessarily produce unacceptable results.

Figures 13 and 14 depict typical patches for plate and solid elements in a severe test for bending action. Results tabulated in table II (ref. 22) show maximum error in stresses for QUAD and HEXA elements. Some observations can be made from this data. HEX8 with linear strain and HEX20 with quadratic strain are conforming elements. As expected, the patch test is not violated. However, the HEX20 with reduced integration, which is nonconforming, passes the test.

Of the plate elements, QUAD2 fails the patch test, because bending rotations in this element are derived from a constant transverse shear strain variation within the element. Thus, it cannot represent a constant curvature state. On the other hand QUAD4 exhibits both force and moment convergence, mainly due to correction terms for transverse shear flexibility imbedded in the formulation. These correction terms do not change the rigid body modes of the element nor do they eliminate the pure shear deformation behavior of the element. They only modify the magnitude of the stiffness coefficients and the locations where the strains are computed. QUAD8 is an isoparametric, conforming element without the above devices to improve its bending behavior. This may account for its poor convergence in table II.

## Effect of Element Distortion

Careful attention should be given to preserving isosceles, square and cube shapes of NASTRAN TRIA, QUAD and HEX elements, respectively. To illustrate the effect of distortion in NASTRAN elements, figure 15 displays three untwisted cantilever beams with different mesh arrangements. The geometric dimensions, material parameters and load conditions are shown in the figure. In the first case the elements are undistorted. This case is designated as a regular mesh (Reg) arrangement. For the second case the elements sides are skewed at a 45° angle to form trapezoidal shape elements in the first of two irregular mesh (IRReg) arrangements. Finally, the last case shows an IRReg arrangement of parallelogram shape elements with sides also skewed at 45°.

Normalized displacement response at the beam tip is tabulated in table III for extensional, flapwise bending, edgewise bending and torsional modes. Some observations can be drawn from the numerical data. First, the extensional and torsional modes are independent of element distortion. Identical results were obtained for the regularly and irregularly-shaped elements. This is indicated in table III by the (BOTH) notation. Second, the change in results between the two IRReg arrangements is negligible. Third, MSC's QUAD4 seems to show a mark degradation of accuracy in the flapwise bending mode of IRReg models, while its three-dimensional cousin, HEXA8, exhibits an error in both the flapwise and edgewise bending modes. In a paper on QUAD4's formulation (ref. 23), the author cites this effect of element distortion: "After the paper was submitted for publication, it was discovered that large errors occur when the skew angle of the element exceeds 20°. This error was traced to coupling between transverse shear strains, and has subsequently been corrected" (1978). Apparently, this deficiency is still present in QUAD4 as illustrated by these more updated results (ref. 22), and thus, the 20° limit on element skew should be used when using QUAD4 or HEX8.

With the exception of the above remarks, all of the elements in table III display good to excellent convergence. Note that QUAD2, although not shown, performed poorly in the edgewise bending and torsional modes (ref. 22). This deficiency is, again, related to the constant transverse shear strain assumption in the QUAD2 element formulation.

## Cantilever Beam with Sweep

Recently developed propfan blades are highly swept at the tip (approximately 35° in some proposed models (ref. 33)). To illustrate NASTRAN plate/shell and solid element performance on swept blade configurations, consider the curved cantilevered beam shown in figure 16. The beam is curved (or swept) in its own plane with an included angle of 90°. Table IV displays results for two tip load conditions. As expected, the QUAD2 exhibits overstiff results for both directions. But, QUAD4 and HEX20 both show average convergence in the in-plane response direction and good convergence in the out-of-plane direction. Better still, reduced integration forms of HEX20 and QUAD8 portray the best results by far.

## Morley's Simply-Supported Swept Plate (ref. 24).

In June 1983, a user project on sweep effects in plates was proposed in Finite Element News (ref. 25). The investigators received participation from numerous researchers and users. The scope of submitted finite element results revealed 33 plate bending element formulations and employed 19 finite element computer codes. Three finite element mesh densities were requested to test convergence of predicted center point displacements of simply-supported plates. A total of four sweep angles were requested to show distortion sensitivity of the finite elements. This section discusses the MSC/NASTRAN results.

Figure 17 shows a schematic description of the proposed plate model. The series solution developed by Morley (ref. 24) is given in table V. The MSC/NASTRAN results reported (ref. 25) are for the QUAD4 and TRIA3 elements. The triangles are chosen so that all rectangles are cut along the shorter diagonal, as shown in figure 17. At zero sweep, the plate mesh is symmetrical. This ensures a maximum number of triangles at the center point of the plate, where maximum force and response is anticipated.

Numerical data tabulated in tables VI and VII show the percentage error in calculated moment and response of using QUAD4 and TRIA3 elements. These percentage errors are based on Morley's series solution for the maximum and minimum bending moments and the vertical displacement at the plate center. Results for the three mesh conditions are given for sweep angles of 30 to 90° as designated in figure 17. Although the tabulated results show the effects of sweep, they also include the effect of aspect ratio (a/h) (see fig. 17). Since the plate has a constant boundary length (a), the value of h will change for each sweep angle. The aspect ratio for an unswept plate is assumed to be unity. The aspect ratio values increase with sweep angle to a final value of two for 30° sweep.

Additional points can be drawn from the data in tables VI and VII. Generally, with both QUAD4 and TRIA3 element assemblages, an error is apparent for plates with sweep angles between 40 and 60°. As sweep angle is increased, the difference in accuracy of calculated moment and response between the QUAD4 and TRIA3 elements diminish. Intuitively, this is suspected to be an effect of aspect ratio (which is further discussed in a later section). For the larger sweep angles at a given mesh densities, the QUAD4 and TRIA3 elements become quite distorted in shape. This distortion is a major contribution to the error of the predicted results. Thus, it is safe to suggest that a refined mesh yields more accurate results for highly swept plate models. This will yield better-shaped QUAD4 and TRIA3 elements in the mesh.

## Cantilever Beam with Pretwist

A cantilever beam with 90° twist from root to tip is shown in figure 18. Table VIII compares NASTRAN triangle and solid element prediction of displacement response at the beam tip for two bending directions. All elements performed quite well for each response mode with TRIA6 and reduced integration form of HEX20 as particular standouts.

## Element Aspect Ratio and Modified Integration

An indirect effect of element aspect ratio is shown by the normalized deflection response data for a quarter-plate mesh of NASTRAN's QUAD or HEX elements in figure 19 and table IX. Plate aspect ratios of 1 and 5 are used as example test cases. Note that the HEX20, shows poor results for the very coarse meshes. However, the HEX20R improves these results very significantly. The HEX20R stiffness coefficients are calculated by modifying the evaluation of strain energy in the HEX20. The essential difference here is that the number and location of the integration points used within the element to evaluate the shear strain energy terms are chosen differently. Details of this technique are inappropriate here, however, the basic idea can be explained by referring to the isoparametric quadrilateral in figure 20.

It can be seen (fig. 20(b)) that an actual residual bending occurs due to transverse shear action, when the element is subjected to a pure bending stress. This residual bending becomes very significant as the aspect ratio of the element is increased. The assumed displacement functions require that the element edges remain straight under pure bending (solid lines), where in fact, the edges should be curved (dashed lines). If the transverse shear effect were omitted the element stiffness representation would be substantially improved. Note that the strain due to pure shear stress (fig. 20(c)) should remain. A practical procedure to obtain the shear strain terms for HEX elements is to use its centroid as the integration point; this neglects the shear strain of figure 20(b), yet retains that of figure 20(c).

The use of modified integration points, chosen so as to suppress undesirable element behavior, is noteworthy. Particularly, it is quite effective in beefing up the bending action of three-dimensional isoparametric elements, when they are used to model thin or moderately thick blade surfaces. This element modification is especially beneficial as the element aspect ratios becomes large. Note that this element improvement device is not fail-safe. Because,

as element aspect ratios become too large, mesh redefinition may be the only alternative approach.

## Cambered Blade and Twisted Blade Vibrations

This section examines benchmark tests for vibration analyses. The cambered compressor blade described in figure 21 was analyzed by MacNeal (ref. 23) in a severe vibration analysis test of QUAD4 elements. The numerical results are tabulated in table X. Eight free vibration modes are given along with some comparative data from Olson and Lindberg (refs. 5 and 29). All modes were predicted extremely well. However, the second mode is a particular stand-out, because its refined results agrees more with Olson's analytical calculations and not with experiment. The probable source of error comes from support compliance in the prediction of the second mode. Because this mode is typically characterized by no surface nodal lines in camber blade configurations, it is difficult to accurately model its support condition.

Although finite element analysis for plate vibrations has become commonplace, "significant differences in the published results for various methods of analysis have raised some doubt concerning the adequacy of these methods to accurately predict the vibratory characteristics of highly twisted cantilever plates," according to Kielb, et al. (ref. 10). They continue to explain, "An example of the types of difference existing in the literature is the predicted first bending frequency for pretwisted plates. The predicted dependency of frequency on twist angle for twisted, cantilever plates spans the spectrum from increasing significantly to decreasing significantly. To be more specific, the trends seen in the literature are: reference 30 - significant increase, references 31 to 33 - slight increase, reference 34 - no change, references 35 and 36 - significant decrease, references 37 and 38 - slight decrease and then an increase, and references 7 and 39 - significant decrease."

Two proposed TRIA2 and QUAD4 grids for the twisted plate model in figure 22 were recently submitted to a finite element users project (refs. 10 to 12). The TRIA2 grid is shown for a plate of aspect ratio (a/b) equal to 1 and a total plate twist of 45°. A total of 360 DOF and 128 elements are used with 9 nodes in the spanwise and chordwise directions. A lumped mass formulation is utilized. The QUAD4 grid represents a plate with a/b = 3 and a total twist of 60°. A total of 550 DOF and 100 elements are used with 11 nodes in the spanwise and chordwise directions. A consistent mass formulation is employed. Figure 22 also shows the dependence of frequency parameter on twist angle for a/b = 1 only. The results of the TRIA2 and QUAD4 elements and those of experiment are highlighted over the finite elements results used by other investigators. It is apparent that the predicted first bending frequency variation is significantly increasing for the TRIA2 model (highlighted with dots), whereas the trend for the QUAD4 model is significantly decreasing (highlighted with stars). Note that the two experimental results (shown as dotted lines) depict a significantly decreasing trend. In all modes shown, the TRIA2 models is predicting overly-stiff results compared to those of the QUAD4 model.

## Summary of Test Results

An attempt has been made to grade the TRIA, QUAD and HEX elements in their performance in the above tests. The results are given in tables XI and XII. An average rating and an approximate grade for each element is compiled at the bottom of the table. Based on the judgments of the author, QUAD4 and TRIA3 exhibited the best overall performance and is the recommended choice amongst the NASTRAN plate elements for practical blade applications. Both of these elements pass the patch test, which ensures (in the limit) convergence of solution. Of the NASTRAN solids examined, HEX20 with modified integration performed the best and is highly recommended for three-dimensional analysis of thin or moderately thick blade planforms.

## CO-PLANAR SHELL ELEMENTS IN NASTRAN

While using NASTRAN shell elements, undesirable difficulties arise when these elements are joined at finite angles. This element joining is commonly referred to as "co-planar elements." The problem is especially acute, while the blade is loaded and deformed during particular subcases of NASTRAN SOLUTION 64 (large displacement analysis). Essentially, a surplus of degrees of freedom (DOF) corresponding to an in-plane rotation originates in the transformation phase of NASTRAN shell elements and can cause singularity of the global stiffness matrix. What results is a solution that either requires a large number of subcases for convergence or leads to nonconvergence.

To clarify this point, consider the example shown in figure 23. Here, representative triangular elements have individual nodal parameters corresponding to membrane and bending actions. If the triangles are not co-planar in an assembly, the common node A is capable of resisting 6 independent responses, when the nodal parameters are transformed into global coordinates. However, if the elements are co-planar, only 5 DOF will exist and thus, global transformations will create zero stiffness coefficients in the sixth DOF. The TRIA3 and QUAD4 elements are more likely to have co-planar difficulties than the TRIA6 and QUAD8, since the midside nodes ensure better compatibility of the local normals of adjacent elements.

To overcome this source of difficulty, a variety of practical procedures have been used in the analysis of arbitrary shells. An indirect approach involves taking, as the normal, the average of the normal directions associated with each of the elements connected at a particular node of the shell. When the element stiffness has been transformed to the global system, the sixth DOF is eliminated by deleting the corresponding row and column from the global stiffness matrix. Eliminating this DOF is equivalent to constraining the shell structure against this motion.

Physically, the shell is quite stiff in this normal rotation, so the imposed constraint has a negligible effect on its response. This point is clarified by the data in table XIV. A cylindrical shell is clamped at one end (fig. 24), and allowed to deflect under its own weight (ref. 41). Five different lengths are considered, ranging from 25 to 200 ft. Plane quadrilateral shell elements are used with meshes having 5 nodes in the circumferential direction and 6 to 11 nodes in the spanwise direction, depending on the shell

length. The computed vertical deflections at the free end show that for the very flexible shell configuration, the effect of the sixth DOF constraint is negligible.

A more direct remedy to the co-planar element problem is to insert an arbitrary stiffness coefficient in the sixth DOF of the element stiffness matrix. After transformation to the global system, a perfectly well-behaved set of equations is achieved from which, all displacements and stress resultants, including those corresponding to the sixth DOF, are obtained. A fictitious set of normal rotation stiffness coefficients for triangular shell elements (table XV) have been suggested by Zienkiewicz (ref. 42). Similar matrix terms can be added for rectangular elements. These additional terms are far better than just placing small terms on the diagonal, because they pass the patch test, when added to the element stiffness matrix. Like the first method, the effect of these fictitious springs on calculated results is negligible.

A new parameter card K6ROT exists in MSC/NASTRAN (versions 63 and higher) that does this automatically. Actually, for QUAD4 and TRIA3 only, the added artificial stiffness coefficients are similar to those of reference 42. A recently completed study (ref. 43) revealed that values of the parameter K6ROT of 1000, 10 000 and 100 000 alleviated the singularity problems and gave smoother responses for advanced turboprop blade models on an element-toelement and node-to-node basis.

Figure 25 displays strain gage locations and two finite element grids (using QUAD4 and TRIA3) for a SR-3C-3 propfan blade, which was analyzed in the study of reference 43. The value of K6ROT was varied to show that frequencies and response are not significantly changed with the variation of this artificial plate normal stiffness. It was also noted that predicted strains were not significantly affected by changes in K6ROT. Additionally shown in the study was that the element-to-element strain variations became much "smoother" when the triangles were made more nearly equilateral or when the triangles were eliminated and QUAD4 elements were used (fig. 25).

Table XVI presents frequency results for the QUAD4 grid model at 0 rpm using K6ROT = 0, 10 000 and 100 000. A faster convergence rate to a steady-state response of the blade is observed with K6ROT = 10,000, where a total of 6 subcases were needed in NASTRAN Solution 64, instead of 25 subcases (with K6ROT = 0). Additionally, increased values of the K6ROT parameter resulted in small changes in the calculated modes. NASTRAN runs using K6ROT = 10,000 with TRIA3 are also shown in table XVI. Strain gage results for the propfan blade rotating at a speed of 8508 rpm are given in table XVII. Strain gage locations are shown in figure 25. Gage 1 measured a strain in the radial direction of the blade. At gage 2 a strain was measured in the circumferential direction, while a shear strain was measured at gage 3. Again, measured strains at the gage points of both the QUAD4 and TRIA3 elements were not significantly affected by changes in the K6ROT parameter.

From the study (ref. 43) it was concluded that the use of K6ROT to add artificial plate normal stiffness significantly reduced element-to-element strain variations in the finite element models of the flexible blades examined. Additionally the nonlinear steady state solution converged much faster than when alternative procedures were used. A value of K6ROT = 10,000 was shown to give good results for the practical blade models.

A companion memorandum (ref. 44) gives specific NASTRAN data instructions on the use of PARAMeter card K6ROT.

## EFFECT OF CENTRIFUGAL STIFFENING AND SOFTENING FORCES

Consider a straight cantilever blade undergoing bending vibrations perpendicular to the plane of rotation. The centrifugal tensile force tends to stiffen the transverse bending elastic springs. In vibration analysis, this force generally increases the square of the natural frequencies in proportion to the square of the rotation speed. The constant of proportionality is known as the Southwell coefficient (ref. 1). Centrifugal stiffening effects are placed in the finite element formulation through supplemental strain energy terms due to the initial stress of steady-state rotation.

In a rotating reference frame, there is an additional force that acts in the radial and circumferential directions of the blade. As a mass point displaces radially outward, there is an effective increase in the total magnitude of centrifugal force carried by this point that is proportional to its total displacement. When this effective centrifugal force increase is algebraically added to the incremental elastic stiffness (i.e., brought from the right-hand to the left-hand side of the equation of motion), a reduction in elastic stiffness of the system is apparent. This stiffness reduction is called "centrifugal softening." In vibration analysis, this force has the effect of reducing the natural frequencies. Centrifugal softening effects are incorporated in the finite element formulation by subtracting the mass times the square of the rotational speed from the stiffness matrix (see ref. 44 for detailed formulations).

To illustrate the effect of the centrifugal stiffening and softening forces, consider the flat cantilever blade with length ratio equal to 3. The axis of rotation is placed at the root section. This problem is the second of two phases of a joint research effort on vibrations of twisted blades (refs. 10 to 12). Tables XVIII and XIX each show five sets of submitted results of nondimensional frequencies for the first five modes at three-nondimensional rotation speeds (0,2,6). For the results in table XVIII, all mass points of the plate are spinning in the plane of rotation, whereas a 90° setting angle of the plate is assumed for the cases of table XIX.

As expected, an apparent increase in the frequency parameter is observed as a result of the centrifugal stiffening effect due to rotation. Investigators A,C and D included centrifugal softening in their formulations. Investigators B and E omitted this effect. From the numerical trends in table XVIII, it is quite obvious that the centrifugal softening effect is essential to the accuracy of frequency calculations of rotating blades. With a 90° angular rotation of the plate, the centrifugal softening effect disappears. Thus, this effect is dependent on the blade's setting angle at the axis of rotation (or root section).

The question of inserting centrifugal softening terms in a NASTRAN run of a practical blade is important, especially when large displacement effects are considered. NASTRAN specific data instructions for insertion of these terms are inappropriate to discuss herein. These aspects are dealt with in reference 44.

## EFFECT OF CORIOLIS FORCES

In addition to the centrifugal stiffening and softening forces present in rotating blades, there exist Coriolis forces that affect the blade response at relatively high rotation speeds. Coriolis forces are produced when a mass point of the blade displaces relative to a rotating reference frame. These forces are perpendicular to the plane containing the rotation axis of the blade and the instantaneous velocity vector of the mass point. They are proportional to the vibratory velocities, but unlike viscous damping forces, are path-independent in nature. In a finite element formulation, the contrast between Coriolis and damping forces is the skew-symmetric versus symmetric form of their matrices.

Many investigators have considered Coriolis forces in their blade vibration analyses and have commented on the significance and importance of this effect. One such work is that of Sreenivasamurthy and Ramamurti (ref. 47) in the effect of Coriolis forces on rotating plates. Here, triangular plate finite elements with uncoupled membrane and bending stress behaviors were utilized. Their results showed that for a uniform thick plate of aspect ratio equal to one and rotating at a speed near the first nonrotating frequency, the first bending and torsional frequencies decreased by 3.23 and 8.02 percent respectively, due to Coriolis forces. The overall effect of these forces were most significant for plate setting angles of 45°. The authors stated that for plates rotating at high speeds inclusion of Coriolis forces in the computation of natural frequencies is desirable.

However, upper bound solutions for the free vibrations of rotating cantilever plates have recently been reported by Co (ref. 48). For thin plates of aspect ratio equal to one, Co found the most significant change in the fundamental mode due to Coriolis terms to be less than 0.1 percent at a rotation speed equivalent to three times the nonrotating frequency. It was also noted that by increasing the plate thickness the Coriolis effect increases, but no more than 1 percent for the fundamental mode.

The Ritz method utilized in reference 48 provides upper bound solutions. Generally, the significance of Coriolis forces arises at very high rotation speeds of thicker blades mounted at high root setting angles. Modern propfan blades operate at more realistic rotation speeds and do not fall into this category. Thus, in these blades Coriolis effects are typically small and negligible.

## LUMPED VERSUS CONSISTENT MASS MATRICES

The mass matrix formulation in NASTRAN is lumped unless the analyst requests the consistent formulation by means of a PARAM COUPMASS Bulk Data card.

In a lumped mass formulation inertia properties are assigned to the translational and rotational DOF only. The total mass in each element is distributed to the nodal points in an averaging-type of fashion, depending on the element type. In consistent mass formulations the mass matrix is calculated with the same approximating functions used in the stiffness formulation. That is why the word "consistent" is used. Imposed constraints used in the stiffness formulation are progressively applied in a consistent mass formulation.

Therefore, it is suggested that a lumped mass be used with nonconforming elements and a consistent mass with conforming elements.

## CLOSING REMARKS

Progress toward reliable and efficient finite element procedures for rotating, flexible blade structures can best be described as uneven. A major reason for the slow rate of development is the conceptual challenge facing blade analysts in using the finite element method to approximate the blade's deformation behavior under static and dynamic loads.

To address the above challenge, blade analysts can use this manual as a preliminary reference tool. Comparisons are made between NASTRAN plate/shell and solid elements through published benchmark tests that are applicable for studying different blade related parameters such as twist, sweep and camber. The purpose of this report is to provide a summary of blade modeling strategies and to document capabilities and limitations of various NASTRAN elements. The question of implementing the NASTRAN capabilities for practical blades is also important in the intended application to large displacement and frequency analyses, where substantially more complex finite element modeling strategies must be dealt with. These aspects are taken up in a companion report (ref. 44).

## REFERENCES


1. Rao, J.S.; and Carnegie, W.: Effect of Pretwist and Rotation of Flexural Vibrations of Cantilever Beams Treated by Extended Holzer Method. Bull. Mech. Eng. Education, vol. 10, no. 239, 1971.

2. Rao, J.S.: Flexural Vibrations of Turbine Blades. Arch. Budowy Masz., vol. 16, no. 3, 1970, p. 375.

3. Dawe, D.J.: A Finite Element Approach to Plate Vibration Problems. J. Mech. Eng. Sci., vol. 7, no. 1, Mar. 1965, pp. 28-32.

4. Anderson, R.G.; Irons, B.M.; and Zienkiewicz, O.C.: Vibration and Stability of Plates Using Finite Elements. Int. J. Solids Struct., vol. 4, no. 10, 1968, pp. 1031-1055.

5. Olson, M.D.; and Lindberg, G.M.: A Finite Cylindrical Shell Element and the Vibration of a Curved Fan Blade. NRC-LR-497, National Research Council of Canada, Feb. 1968.

6. Dokainish, M.A.; and Rawtani, S.: Bending of Pretwisted Cantilever Plates. Canadian Aeronautics and Space Institute Trans., vol. 2, no. 2, Sept. 1969, pp. 89-94.

7. Dokainish, M.A.; and Rawtani, S.: Vibration Analysis of Pretwisted Cantilever Plates. Canadian Aeronautics and Space Institute Trans., vol. 2, no. 2, Sept. 1969, pp. 95-100.

8. NASTRAN Theoretical Manual. NASA SP-221(06), 1977.

9. Schaeffer, H.G.: MSC/NASTRAN Primer - Static and Normal Modes Analysis. Schaeffer Analysis Inc., 1979.

10. Kielb, R.E.; Leissa, A.; and MacBain, J.C.: Vibrations of Twisted Cantilever Plates - A Comparison of Theoretical Results. Int. J. Numer. Methods Eng., vol. 21, no. 8, Aug. 1985, pp. 1365-1380.

11. MacBain, J.C.; Kielb, R.E.; and Leissa, A.: Vibrations of Twisted Cantilever Plates - Experimental Investigation. J. Eng. Gas Turbines Power, vol. 107, no. 1, Jan. 1985, pp. 187-196.

12. Leissa, A.W.; MacBain, J.C.; and Kielb, R.E.: Vibrations of Twisted Cantilever Plates - Summary of Previous and Current Studies. J. Sound Vibr., vol. 96, no. 2, Sept. 22, 1984, pp.159-173.

13. Srinivasan, A.V.; and Fulton, G.B.: Advanced Turboprop Vibratory Characteristics. (R84-956627-1, United Technologies Research Center; NASA Contract NAS3-23533) NASA CR-174708, 1984.

14. Clough, R.W.; and Wilson, E.L.: Dynamic Finite Element Analysis of Arbitrary Thin Shells. Comput. Struct., vol. 1 nos. 1-2, Aug. 1971, pp. 33-56.

15. Zienkiewicz, O.C.; Taylor, R.L.; and Too, J.M.: Reduced Integration Techniques in General Analysis of Plates and Shells. Int. J. Numer. Methods Eng., vol. 3, no. 2, Apr.-June 1971, pp. 275-290.

16. Iron, B.M.R.; and Hellen, T.K.: On Reduced Integration in Solid Isoparametric Elements When Used in Shells with Membrane Modes. Int. J. Numer. Methods Eng., vol. 10, no. 5, 1975, pp. 1179-1182.

17. Pawsey S.F.: Analysis of Moderately Thick to Thin Shells by Finite Element Method. Ph.D. Thesis, Univ. of California, Berkeley, 1970.

18. Clough, R.W.; and Tocher, J.L.: Finite Element Stiffness Matrices for Analysis of Plate Bending. Matrix Methods in Structural Mechanics, AFFDL-TR-66-80, 1965, pp. 515-545. (Avail. NTIS, 67N22817).

19. Clough, R.W.; and Felippa, C.A.: A Refined Quadrilateral Element for the Analysis of Plate Bending. 4th International Congress on the Application of Mathematics in Engineering, 1968, pp. 399-440.

20. Clough, R.W.; and Johnson, C.P.: Finite Element Analysis of Arbitrary Thin Shells. ACI Symp. on Concrete Thin Shells, New York, 1970.

21. Fong, H.H.; and Jones J.W.: An Evaluation of COSMIC/NASTRAN. New And Future Developments in Commercial Finite Element Methods, Robinson and Assoc., Dorset, England, 1981, pp. 324-338.

22. Harder, R.L.: Review of the MacNeal-Harder Linear Static Test Problems. to appear in Finite Elements in Analysis and Design, vol.1, no.1, 1985.

23. MacNeal, R.H.: A Simple Quadrilateral Shell Element. Comput. Struct., vol. 8, no. 2, Apr. 1978, pp. 175-183.

24. Morley, L.S.D.: Skew Plates and Structures. Pergamon Press, 1963, p. 96.

25. Robinson, J.: Skew Effects - Finite Element Method User Project No. 2 - Morley's Simply-Supported Swept Plate Problem. Finite Element News, nos. 1-6, 1983.

26. Bathe, K.J.; Dvorkin, E.; and Ho, L.W.: Our Discrete Kirchoff and Isoparametric Shell Elements for Nonlinear Analysis - An Assessment. Comput. Struct., vol. 16, no. 1-4, 1983, pp. 89-98.

27. Bathe, K.J.; and Dvorkin, E.N.: A Formulation of General Shell Elements - The Use of Mixed Interpolation of Tensorial Components. Int. J. Numer. Methods Eng., to appear, 1987.

28. Bathe, K.J.; and Dvorkin, E.N.: A Four-Node Plate Bending Element Based on Mindlin/Reissner Plate Theory and a Mixed Interpolation. Int. J. Numer. Methods Eng., in press, 1987.

29. Olson, M.D.; and Lindberg, G.M.: Dynamic Analysis of Shallow Shells With a Doubly-Curved Triangular Finite Element. J. Sound Vibr., vol. 9, no. 3, Dec. 8, 1971, pp. 299-318.

30. Bridle, M.D.J.: Vibration of Thick Plates and Shells. Ph.D thesis, Univ. of Nottingham, England, 1973.

31. MacBain, J. C.: Vibratory Behavior of Twisted Cantilevered Plates. J. Aircr., vol. 12 no. 4, Apr. 1975, pp. 343-349.

32. Ucmaklioglu, M.: Vibration of Shells with Applications to Hollow Blading. PhD. thesis, Univ. of Durham, 1978.

33. Peterson, M.R., et al.: Three-Dimensional Finite-Element Techniques for Gas Turbine Blade Life Prediction. Stresses, Vibrations, Structural Integration and Engine Integrity, AGARD-CP-248, AGARD, France, 1979, pp. 9-1 to 9-14.

34. Toda, A.: An Investigation of Flexural Vibrations of Pretwisted Rectangular Plates. MS. Thesis, Ohio State Univ., 1971.

35. Walker, K.P.: Vibrations of Cambered Helicoidal Fan Blades. J. Sound Vibr., vol 59, no 1, July 8, 1978, pp. 35-57.

36. Thomas, J.; and Soares, C.A.M.: Finite Element Analysis of Rotating Shells. ASME Paper 73-DET-94, Sept. 1973.

37. Petricone, R.D.: Vibration Characteristics and Deformation Due to Centrifugal Loading of Low-Aspect Ratio Compressor Blades. Ph.D thesis, Steven Institute of Technology, Hoboken, N.J., 1970.

38. Petricone, R.; and Sisto, F.: Vibration Characteristics of Low Aspect Ratio Compressor Blades. J. Eng. Power, vol. 93, no. 1, Jan. 1971, pp. 103-112.

39. Sreenivasamurthy, S.; and Ramamurti,.V.: Effect of a Tip Mass on the Natural Frequencies of a Rotating Pre-Twisted Cantilever Plate. J. Sound Vibr., vol. 70, no. 4, June 22, 1980, pp. 598-601.

40. Irons, B.M., et al.: Triangle Elements in Bending - Conforming and Non-Conforming Solutions. Matrix Methods in Structural Mechanics, J.S. Przemieniecki, ed., AFFDL-TR-66-80, 1965, pp. 547-576. (Avail. NTIS, AD-646300).

41. Yeh, C.H.: Large Deflection Dynamic Analysis of Thin Shells Using the Finite Element Method. Ph.D. Thesis, University of California, Berkeley, 1970.

42. Zienkiewicz, O.C., et al.: Arch Dams Analyzed by a Linear Finite Element Shell Solution Program. Proc. Symp. Arch Dams, Inst. Civ. Eng., London, 1968.

43. Arseneaux, P.J.: Resolution of Irregularities with SR-3C and SR-2C Advanced Turboprop Blade Response Finite Element Models. Hamilton Standard Division, unpublished communique.

44. Lawrence, C., et al.: A NASTRAN Primer for the Analysis of Rotating Flexible Blades. NASA TM-89861, 1987.

45. Lawrence, C.; and Kielb, R.E.: Nonlinear Displacement Analysis of Advanced Propeller Structures Using NASTRAN. NASA TM-83737, 1984.

46. Ahmad, S.; Irons, B.M.; and Zienkiewicz, O.C.: Analysis of Thick and Thin Shell Structures by Curved Finite Elements. Int. J. Numer. Methods Eng., vol. 2, no. 3, July-Sept. 1970, pp. 419-451,

47. Sreenivasamurthy, S.; and Ramamurti, V.: A Parametric Study of Vibration of Rotating Pre-Twisted and Tapered Low Aspect Ratio Cantilever Plates. J. Sound Vibr., vol. 76, no. 3, June 8, 1981, pp. 311-328.

48. Co, C.J.: Coriolis Effects on the Vibrations of Rotating Beams, Plates and Shells. Ph-D Dissertation, Ohio State University, 1984.

TABLE I. - RESULTS FOR SCORDELIS-LO SHELL

| Number of node spaces per edge of model | Normalized vertical deflection at midpoint (B) of free edge | | | | | |
|---|---|---|---|---|---|---|
| | QUAD2 | QUAD4 | QUAD8 | HEXA(8) | HEX20 | HEX20(R) |
| 2 | 0.784 | 1.376 | 1.021 | 1.320 | 0.092 | 1.046 |
| 4 | .665 | 1.050 | .984 | 1.028 | .258 | .967 |
| 6 | .781 | 1.018 | 1.002 | 1.012 | .589 | 1.003 |
| 8 | .854 | 1.008 | .997 | 1.005 | .812 | .999 |
| 10 | .897 | 1.004 | .996 | ----- | ----- | ----- |

TABLE II. - PATCH TEST RESULTS

| | Maximum error in stress, percent | | | | | |
|---|---|---|---|---|---|---|
| | QUAD2 | QUAD4 | QUAD8 | HEXA(8) | HEX20 | HEX20(R) |
| Constant-stress loading | 0 | 0 | 18 | 0 | 0 | 0 |
| Constant-curvature loading | 30.7 | 0 | 51.6 | N/A | N/A | N/A |

TABLE III. - RESULTS FOR UNTWISTED CANTILEVER BEAM

[Reg. = No element distortion, IRReg. = element distortion.]

| Mode (Mesh) | Normalized response at beam tip | | | | |
|---|---|---|---|---|---|
| | QUAD4 | QUAD8 | HEX20 | HEXA8 | HEX20(R) |
| Extension (Both) | 0.996 | 0.999 | 0.995 | 0.989 | 0.994 |
| Flapwise (Reg.) | .904 | .987 | .923 | .981 | .966 |
| Flapwise (IRReg.) | .752 | .971 | .967 | .746 | .927 |
| Edgwise (Reg.) | .986 | .991 | ----- | ----- | ----- |
| Edgewise (IRReg.) | .973 | .992 | .916 | .653 | .931 |
| Torsion (Both) | .946 | .953 | 1.020 | .910 | .904 |

TABLE IV. - RESULTS FOR CANTILEVER BEAM WITH SWEEP

| Tip loading direction | Normalized tip displacement in direction of load | | | | | |
|---|---|---|---|---|---|---|
| | QUAD2 | QUAD4 | QUAD8 | HEXA8 | HEX20 | HEX20(R) |
| In-plane (vertical) | 0.025 | 0.833 | 1.007 | 0.880 | 0.875 | 1.006 |
| Out-of-plane | .594 | .951 | .971 | .849 | .946 | .959 |

R - Reduced integration.

TABLE V. - MORLEY'S SERIES SOLUTION (REF. 24)

[$w_c = \alpha x 10^{-3}$;
$^{a}M_{max} = \beta x 10^{-2}$;
$^{a}M_{min} = \gamma x 10^{-2}$.]

| Angle, $\delta$ | Series solution | | |
|---|---|---|---|
| | $\alpha$ | $\beta$ | $\gamma$ |
| 90° | ------ | ---- | ---- |
| 80° | 1.4087 | 4.86 | 4.48 |
| 60° | .9318 | 4.25 | 3.33 |
| 40° | .3487 | 2.81 | 1.80 |
| 30° | .1485 | 1.91 | 1.08 |

[a]The principal bending moments are given by

$M_{max} = M_a + M_b$ and
$M_{min} = M_a - M_b$ where
$M_a = 1/2(M_x + M_y)$ and
$M_b = [1/4(m_x - M_y)^2 + M_{xy}^2]^{1/2}$

TABLE VI. - PERCENTAGE ERROR IN Wc - BASED ON SERIES SOLUTION (REF. 25)

| Angle, δ | Mesh | MSC/NASTRAN | |
|---|---|---|---|
| | | QUAD4 | TRIA3 |
| 90° | 4x4 | ------- | ------ |
| | 8x8 | ------- | ------ |
| | 14x14 | ------ | ------ |
| 80° | 4x4 | -2.68 | -10.13 |
| | 8x8 | .09 | -2.82 |
| | 14x14 | .16 | -.97 |
| 60° | 4x4 | -9.74 | -17.15 |
| | 8x8 | -3.63 | -6.95 |
| | 14x14 | -2.12 | -3.52 |
| 40° | 4x4 | -24.00 | -35.76 |
| | 8x8 | -16.26 | -19.41 |
| | 14x14 | -12.53 | -13.11 |
| 30° | 4x4 | -29.97 | -47.47 |
| | 8x8 | -25.93 | -29.29 |
| | 14x14 | -21.88 | -21.88 |

TABLE VII. - PERCENTAGE ERROR IN $M_{max}$ - BASED ON SERIES SOLUTION (REF. 25)

| Angle, δ | Mesh | MSC/NASTRAN | |
|---|---|---|---|
| | | QUAD4 | TRIA3 |
| 90° | 4x4 | ------ | ------ |
| | 8x8 | ------ | ------ |
| | 14x14 | ------ | ------ |
| 80° | 4x4 | -17.04 | -24.24 |
| | 8x8 | -4.38 | -6.34 |
| | 14x14 | -1.50 | -2.16 |
| 60° | 4x4 | -20.54 | -25.52 |
| | 8x8 | -6.23 | -7.60 |
| | 14x14 | -2.54 | -3.06 |
| 40° | 4x4 | -31.67 | -35.12 |
| | 8x8 | -15.20 | -14.59 |
| | 14x14 | -9.43 | -8.90 |
| 30° | 4x4 | -39.53 | -42.56 |
| | 8x8 | -23.19 | -20.68 |
| | 14x14 | -13.19 | -14.50 |

TABLE VIII. - RESULTS FOR CANTILEVER BEAM WITH PRETWIST[a]

| Tip loading direction | Normalized response at beam tip | | | | |
|---|---|---|---|---|---|
| | TRIA3 | TRIA6 | HEX20 | HEXA8 | HEX20(R) |
| Flapwise | 0.993 | 0.998 | 0.985 | 0.977 | 0.995 |
| Edgewise | .985 | .998 | .995 | .983 | .991 |

[a]Triangular elements used as recommended by NASTRAN (NO element distortions).

TABLE IX. - RESULTS SHOWING EFFECT OF ASPECT RATIO

(a) Aspect ratio = 1.0

| Number of node spaces[a] per edge of model | Normalized lateral deflection at center | | | | |
|---|---|---|---|---|---|
| | QUAD4 | QUAD8 | HEXA8 | HEX20 | HEX20(R) |
| 2 | 0.981 | 0.927 | 0.989 | 0.023 | 1.073 |
| 4 | 1.004 | .996 | .998 | .738 | .993 |
| 6 | 1.003 | .999 | .999 | .967 | 1.011 |
| 8 | 1.002 | 1.000 | 1.000 | .991 | 1.008 |

(b) Aspect ratio = 5.0

| Number of node spaces[a] per edge of model | Normalized lateral deflection at center | | | | |
|---|---|---|---|---|---|
| | QUAD4 | QUAD8 | HEXA8 | HEX20 | HEX20(R) |
| 2 | 1.052 | 1.223 | 0.955 | 0.028 | 1.139 |
| 4 | .991 | 1.003 | .978 | .691 | .995 |
| 6 | .997 | 1.000 | .990 | 1.066 | 1.024 |
| 8 | .998 | 1.000 | .995 | 1.026 | 1.006 |

[a]For elements with midside nodes, the number of elements per edge of model is equal to one-half the number of node spaces.

TABLE X. - VIBRATION RESULTS FOR CAMBERED COMPRESSOR BLADE (REF. 23)

| Mode | Symmetry | Frequency, Hz | | | | | |
|---|---|---|---|---|---|---|---|
| | | Number of elements | | | | Test ref. 5 | Olson ref. 5 |
| | | 2 | 8 | 16 | 32 | | |
| 1 | A | 67.5 | 56.8 | 86.0 | 86.0 | 86.6/85.6 | 86.6 |
| 2 | S | 109.6 | 139.1 | 136.6 | 139.5 | 135.5/134.5 | 139.2 |
| 3 | S | 883.8 | 279.2 | 272.4 | 253.7 | 259 | 251.5 |
| 4 | A | ----- | 416.6 | 360.6 | 371.0 | 351 | 348.6 |
| 5 | S | ----- | 455.3 | 402.4 | 413.6 | 395 | 393.4 |
| 6 | A | ----- | 672.7 | 640.1 | 564.3 | 531 | 533.4 |
| 7 | A | ----- | ----- | 888.9 | 818.6 | 743 | 752.1 |
| 8 | S | ----- | ----- | 888.8 | 867.5 | 851 | 746.4 |

Physical properties of blade

| | |
|---|---|
| Material: | Sheet steel |
| Thickness: | 0.120 in. |
| Radius of curvature: | 24 in. |
| Length: | 12 in. |
| Width (developed): | 12 in. |

A = Anti-symmetric mode
S = Symmetric mode

TABLE XI. - SUMMARY OF TEST RESULTS FOR NASTRAN PLATE/SHELL ELEMENTS

| Benchmark test | Loading | | Mesh[a] | NASTRAN Plate/shell elements[b] | | | | | |
|---|---|---|---|---|---|---|---|---|---|
| | In-plane | Out-plane | | QUAD2 | QUAD4 | QUAD8 | TRIA3 | TRIA6 | TRIA2 |
| 1. Patch test | * | | IRReg. | 4 | 4 | 2 | 4 | 2 | 4 |
| 2. Patch test | | * | IRReg. | 1 | 4 | 1 | 4 | 2 | 1 |
| 3. Straight beam, extension | * | | Both | 4 | 4 | 4 | 4 | 4 | 4 |
| 4. Straight beam, edgewise | * | | Reg. | 0 | 3 | 4 | 2 | 3 | 0 |
| 5. Straight beam, edgewise | * | | IRReg. | 0 | 0 | 3 | 3 | 3 | 3 |
| 6. Straight beam, flapwise | | * | Reg. | 3 | 4 | 4 | 3 | 3 | 3 |
| 7. Straight beam, flapwise | | * | IRReg. | 3 | 3 | 4 | 3 | 4 | 3 |
| 8. Straight beam, twist | (Torque) | | Both | 1 | 3 | 3 | 3 | 3 | 1 |
| 9. Swept beam, edgewise | * | | Reg. | 0 | 2 | 4 | 2 | 2 | 0 |
| 10. Swept beam, flapwise | | * | Reg. | 1 | 3 | 3 | 2 | 2 | 1 |
| 11. Twisted beam | * | * | Reg. | 0 | 4 | 4 | 4 | 4 | 1 |
| 12. (1/4) flat plate | | * | Reg. | 2 | 3 | 3 | 3 | 3 | 2 |
| 13. Scordelis-lo shell | * | * | Reg. | 2 | 3 | 4 | 3 | 3 | 2 |
| 14. Morley's swept plate | | * | IRReg. | - | 2 | - | 2 | - | - |
| 15. Cumbered blade (vibration) | N.A. | N.A. | Reg. | 1 | 4 | - | 3 | - | 2 |
| 16. Twisted plate (vibration) | N.A. | N.A. | Reg. | 0 | 4 | - | 4 | - | 1 |
| | Average rating: | | | 1.40 | 3.13 | 3.31 | 3.06 | 2.92 | 1.87 |
| | Approximate grade: | | | D | B- | B | B- | B- | D+ |

Notes:
[a]"Ref." = element shape not intentionally distorted.
[a]"IRReg." = element shape is intentionally distorted.
[a]"BOTH" = Both "Reg." and "IRReg." mesh used.
[b]4 = Excellent, 3 = Good, 2 = Average, 1 = Poor, 0 = N.G.

TABLE XII. - SUMMARY OF TEST RESULTS FOR NASTRAN SOLID ELEMENTS

| Benchmark test | Mesh[a] | NASTRAN solid elements[b] | | |
|---|---|---|---|---|
| | | HEXA8 | HEX20 | HEX20(MI) |
| 1. Patch test | IRReg. | 4 | 4 | 4 |
| 2. Straight beam, extension | Both | 4 | 4 | 4 |
| 3. Straight beam, flapwise | Reg. | 4 | 3 | 3 |
| 4. Straight beam, edgewise | IRReg. | 0 | 3 | 4 |
| 5. Straight beam, flapwise | IRReg. | 0 | 3 | 3 |
| 6. Straight beam, twist | Both | 3 | 3 | 3 |
| 7. Swept beam, edgewise | Reg. | 2 | 2 | 4 |
| 8. Swept beam, flapwise | Reg. | 2 | 3 | 3 |
| 9. Twisted beam, edgewise/ flapwise | Reg. | 3 | 3 | 4 |
| 10. (1/4) flat plate | Reg. | 3 | 0 | 1 |
| 11. Scordelis-low shell | Reg. | 3 | 0 | 3 |
| 12. Cambered blade (vibrations) | Reg. | 3 | 0 | 3 |
| 13. Twisted plate (vibrations) | Reg. | 4 | 3 | 4 |
| | | ___ | ___ | ___ |
| Average rating: | | 2.7 | 2.4 | 3.3 |
| Approximate grade: | | C+ | C | B |

Notes:

(MI) = with modified integration.
[a]"Reg." = element shape not intentionally distorted.
[a]"IRReg." = element shape is intentionally distorted.
[a]"BOTH" = Both "Reg." and "IRReg." mesh used.

[b]Rating System: 4 = Excellent; 3 = Good; 2 = Average; 1 = Poor; 0 = N.G.

TABLE XIII. - EFFECT OF SIXTH D.O.F. ON DEFLECTION OF SHELL TIP

| Length, ft | Deflection at midpoint of shell tip, ft | | |
|---|---|---|---|
| | 5 DOF | 6 DOF | Percent error |
| 25 | 0.03695 | 0.3696 | 0.03 |
| 50 | .2374 | .2375 | .04 |
| 100 | 1.303 | 1.307 | .31 |
| 160 | 4.501 | 4.509 | .18 |
| 200 | 8.064 | 8.075 | .14 |

TABLE XIV. - FICTITIOUS SET OF NORMAL ROTATION STIFFNESS COEFFICIENTS FOR TRIANGLE SHELL ELEMENTS (REF. 42)

$$\begin{Bmatrix} M_{Z_A} \\ M_{Z_B} \\ M_{Z_C} \end{Bmatrix} = (\alpha EAt) \begin{bmatrix} 1.0 & -0.5 & -0.5 \\ & 1.0 & -0.5 \\ \text{sym.} & & 1.0 \end{bmatrix} \begin{Bmatrix} \theta_{Z_A} \\ \theta_{Z_B} \\ \theta_{Z_C} \end{Bmatrix}$$

where $\alpha$ = arbitrary coefficient

TABLE XV. - MODAL RESULTS FOR SR-3C-3 PROPFAN BLADE AT ZERO RPM (REF. 43)

| Mode | KROT6 with MSC/QUAD4, Hz | | |
|---|---|---|---|
| | 1000 | 10 000 | 100 000 |
| 1 | 203.5 | [a](206.8)<br>203.6 | 204.1 |
| 2 | 444.8 | [a](458.1)<br>445.1 | 446.8 |
| 3 | 663.3 | [a](665.8)<br>663.5 | 664.7 |
| 4 | 815.2 | [a](858.6)<br>816.2 | 821.1 |

[a]KROT6 with MSC/TRIA3.

TABLE XVI. - STRAIN GAGE RESULTS FOR SR-3C-3 PROPFAN BLADE ROTATING AT SPEED OF 8508 RPM (REF. 43)

| Gage | KROT6 with MSC/QUAD4, in./in./in. | | |
|---|---|---|---|
| | 1000 | 10 000 | 100 000 |
| 1 | 380.7 | [a](402)<br>380.4 | 380.0 |
| 2 | 79.5 | [a](85.0)<br>79.4 | 78.9 |
| 3 | 145.1 | [a](174.0)<br>145.3 | 146.7 |

[a]KROT6 with MSC/TRIA3.

TABLE XVII. - VIBRATIONS OF ROTATING TWISTED PLATES (0 DEGREES SETTING ANGLE)

[1B = 1st bending (flap); 1T = 1st torsion; 2B = 2nd bending (flap); 3B = 3rd bending (flap); 1E = 1st bending (edge); Ω = nondimensional rotation speed.]

| Mode/Ω | A | B | C | D | E |
|---|---|---|---|---|---|
| 1B | | | | | |
| 0 | 3.42 | 3.4 | 3.35 | ----- | 3.395 |
| 2 | 4.08 | 4.54 | 4.4 | 4.16 | 4.515 |
| 6 | 7.35 | 9.49 | 7.34 | 7.41 | 9.461 |
| 1T | | | | | |
| 0 | 20.88 | 21.2 | 21.08 | ----- | 20.947 |
| 2 | 21 | 21.3 | 21.2 | 19.56 | 21.258 |
| 6 | 21.8 | 22.9 | 22 | 20.52 | 23.51 |
| 2B | | | | | |
| 0 | 21.31 | 21.7 | 21 | ----- | 21.312 |
| 2 | 22.3 | 22.4 | 22 | 23.03 | 22.428 |
| 6 | 29.2 | 29.8 | 29 | 29.8 | 28.861 |
| 3B | | | | | |
| 0 | 59.79 | 60.1 | 59 | ----- | 60.032 |
| 2 | 60.9 | 61.3 | 60.1 | 62.08 | 61.164 |
| 6 | 68.9 | 69.5 | 68.3 | 65.62 | 69.468 |
| 1E | | | | | |
| 0 | 62.23 | 63.7 | 63.8 | ----- | 62.374 |
| 2 | 62.3 | 63.8 | 63.8 | 62.08 | 62.722 |
| 6 | 62.8 | 64.3 | 64.4 | 64.62 | 62.417 |

TABLE XVIII. - VIBRATIONS OF ROTATING TWISTED PLATES (90 DEGREES SETTING ANGLE)

[1B = 1st bending (flap); 1T = 1st torsion; 2B = 2nd bending (flap); 3B = 3rd bending (flap); 1E = 1st bending (edge); Ω = nondimensional rotation speed.]

| Mode/Ω | A | B | C | D | E |
|---|---|---|---|---|---|
| 1B | | | | | |
| 0 | 3.42 | 3.4 | 3.35 | ----- | 3.4 |
| 2 | 4.54 | 4.54 | 4.49 | 4.16 | 4.04 |
| 6 | 9.5 | 9.49 | 9.48 | 9.53 | 9.32 |
| 1T | | | | | |
| 0 | 20.88 | 21.2 | 21.08 | ----- | 20.95 |
| 2 | 21.2 | 21.5 | 21.4 | 19.76 | 21.06 |
| 6 | 23.4 | 23.7 | 23.6 | 22.2 | 21.94 |
| 2B | | | | | |
| 0 | 21.31 | 21.7 | 20.96 | ----- | 21.31 |
| 2 | 22.4 | 22.4 | 22.1 | 23.12 | 22.34 |
| 6 | 29.8 | 29.8 | 29.6 | 30.4 | 29.25 |
| 3B | | | | | |
| 0 | 59.78 | 60.1 | 59 | ----- | 60.03 |
| 2 | 60.9 | 61.2 | 60.1 | 62.15 | 61.13 |
| 6 | 69.15 | 69.5 | 68.5 | 66.17 | 69.21 |
| 1E | | | | | |
| 0 | 62.23 | 63.7 | 63.8 | ----- | 62.37 |
| 2 | 62.8 | 63.8 | 63.8 | 62.8 | 62.44 |
| 6 | 66.57 | 64.4 | 64.1 | 70.64 | 62.99 |

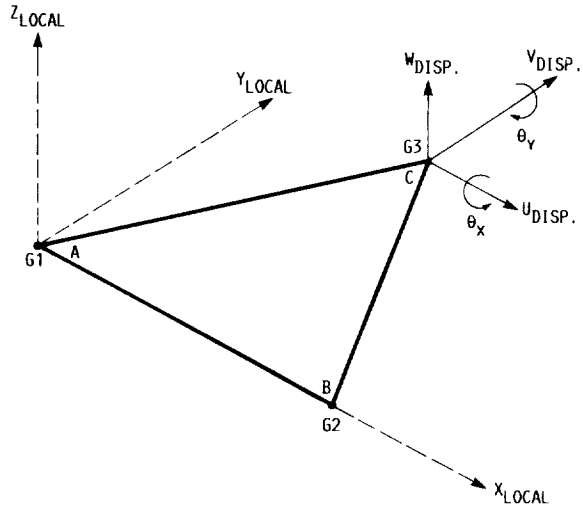


FIGURE 1. - COSMIC NASTRAN's TRIA2.

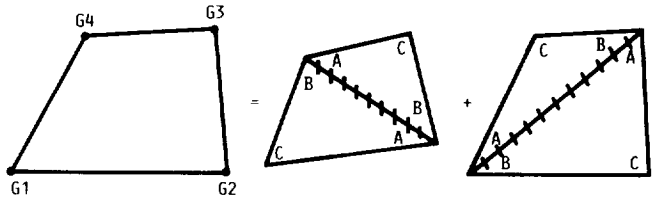


FIGURE 2. - COSMIC NASTRAN's QUAD2.

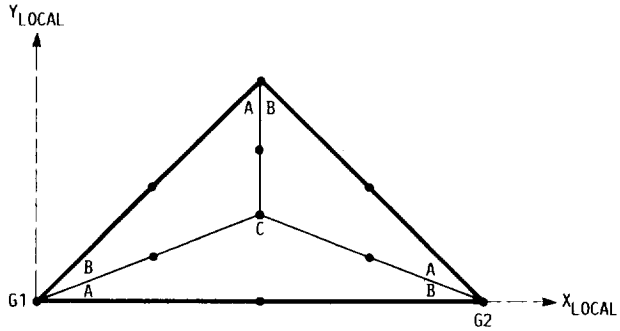


FIGURE 3. - THE CLOUGH TRIANGLE FOR COSMIC/NASTRAN.

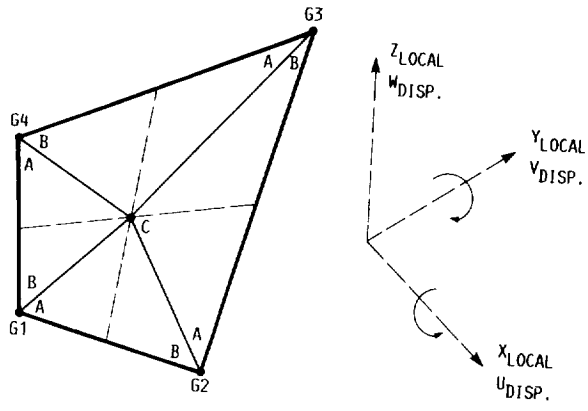


FIGURE 4. - THE SAP SHELL ELEMENT FOR COSMIC/NASTRAN.

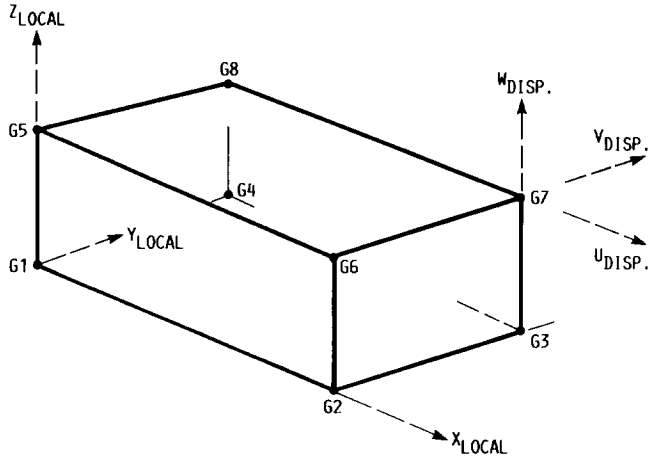


FIGURE 5. - MSC/NASTRAN's HEX8.

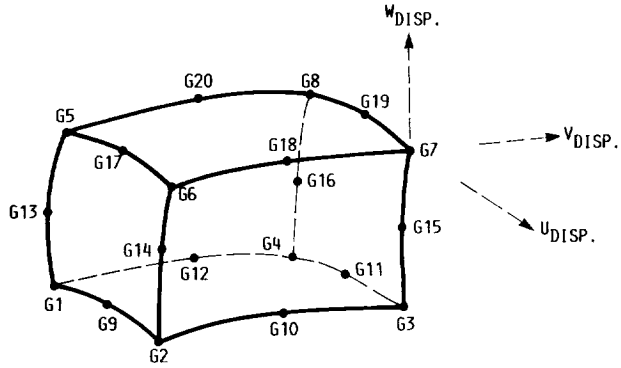


FIGURE 6. - MSC/NASTRAN's HEX20.

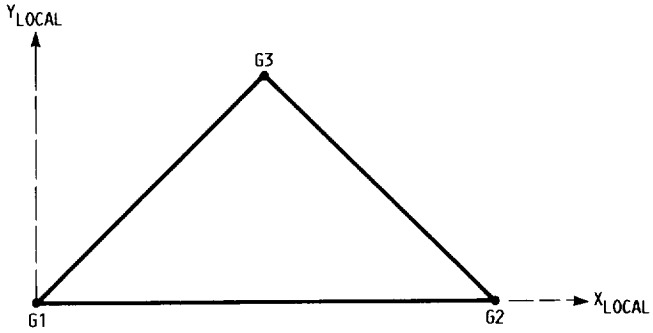


FIGURE 7. - MSC/NASTRAN's TRIA3.

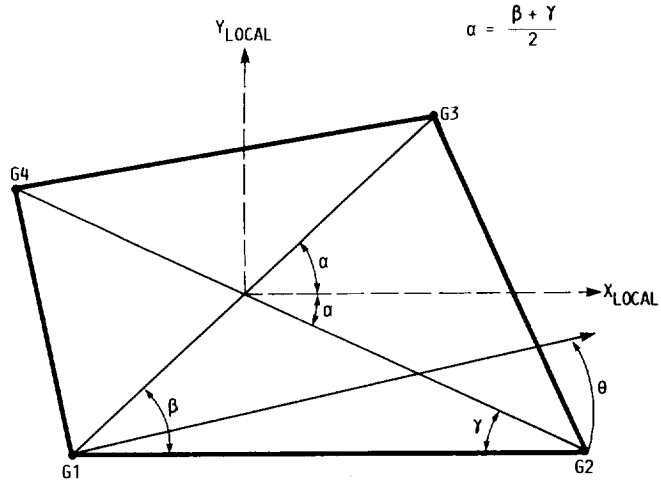


FIGURE 8. - MSC/NASTRAN's QUAD4.

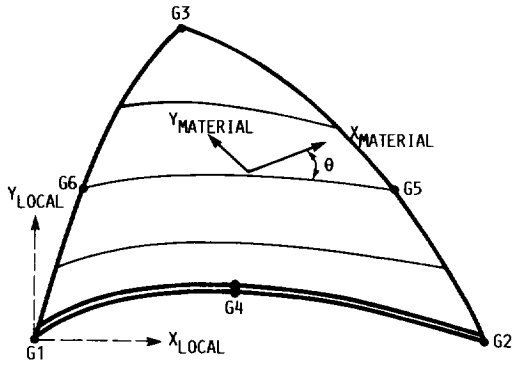


FIGURE 9. - MSC/NASTRAN's TRIA6.

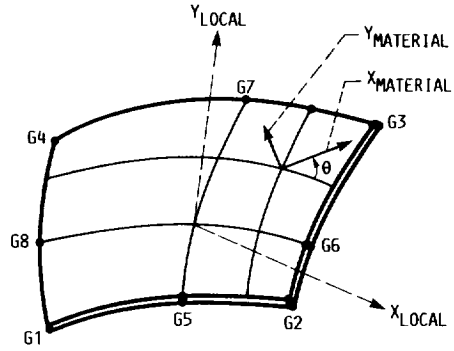


FIGURE 10. - MSC/NASTRAN's QUAD8.

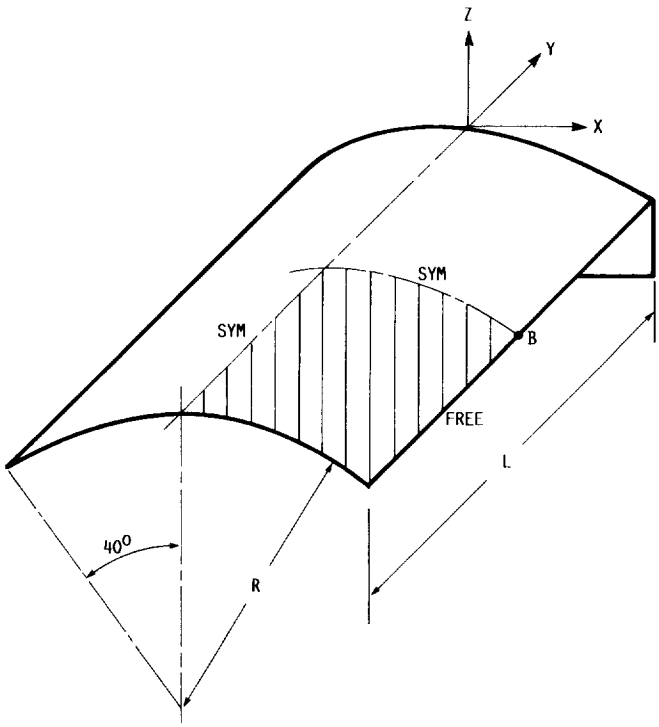


FIGURE 11. - SCORDELIS-LO ROOF. RADIUS = 25.0; LENGTH = 50.0; THICKNESS = 0.25; E = $4.32 \times 10^8$; $\nu$ = 0.0; LEADING = 90.0 PER UNIT AREA IN -Z DIRECTION; $U_x = U_z = 0$ ON CURVED EDGES; MESH: N x N ON SHADED AREA.

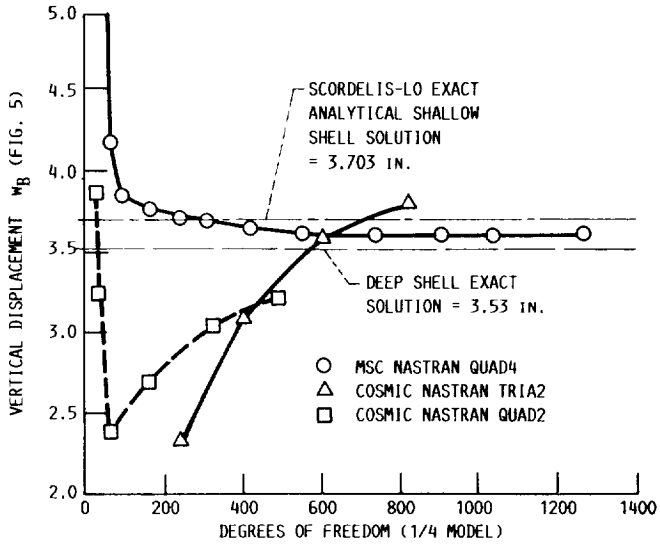


FIGURE 12. - CONVERGENCE OF NASTRAN ELEMENTS IN SCORDELIS-LO ROOF.

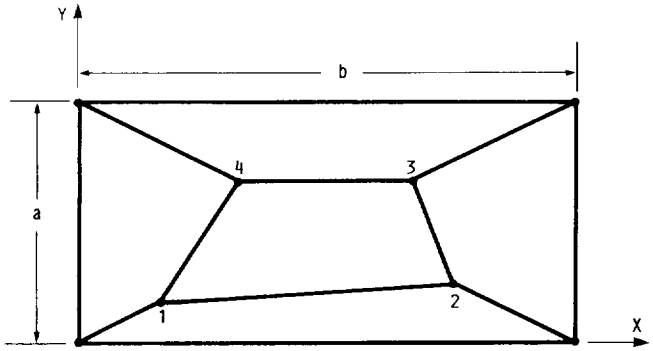


LOCATION OF INNER NODES:

| | X | Y |
|---|---|---|
| 1 | 0.04 | 0.02 |
| 2 | .18 | .03 |
| 3 | .16 | .08 |
| 4 | .08 | .08 |

FIGURE 13. - PATCH TEST FOR PLATES. a = 0.12; b = 0.24; t = 0.001; E = $1.0 \times 10^6$; $\nu$ = 0.25.

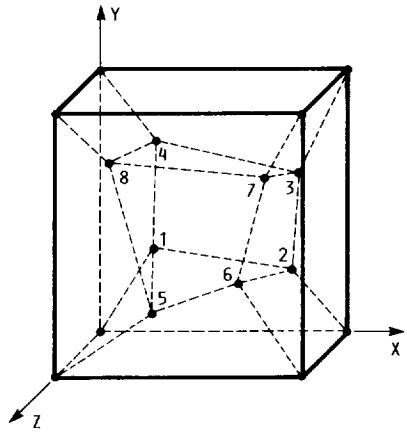


LOCATION OF INNER NODES:

| | X | Y | Z |
|---|---|---|---|
| 1 | 0.249 | 0.342 | 0.192 |
| 2 | .826 | .288 | .288 |
| 3 | .850 | .649 | .263 |
| 4 | .273 | .750 | .230 |
| 5 | .320 | .186 | .643 |
| 6 | .677 | .305 | .683 |
| 7 | .788 | .693 | .644 |
| 8 | .165 | .745 | .702 |

FIGURE 14. - PATCH TEST FOR SOLIDS. OUTER DIMENSIONS: UNIT CUBE; E = $1.0 \times 10^6$; $\nu$ = 0.25.

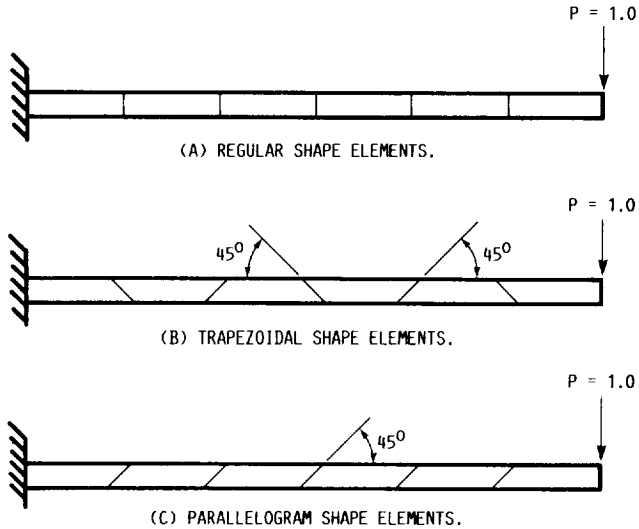


FIGURE 15. - UNTWISTED CANTILEVER BEAM. LENGTH = 6.0; WIDTH = 0.2; DEPTH = 0.1; E = $1.0 \times 10^7$; $\nu$ = 0.30; MESH = 6 x 1; LOADING: UNIT FORCES AT FREE END. NOTE: ALL ELEMENTS HAVE EQUAL VOLUME.

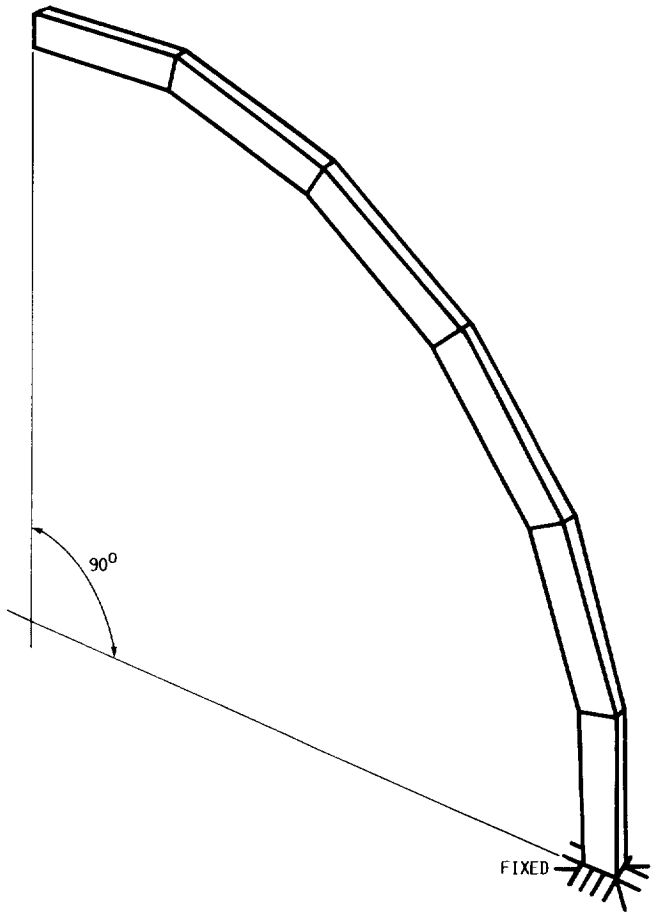


FIGURE 16. - CANTILEVER BEAM WITH SWEEP. INNER RADIUS = 4.12; OUTER RADIUS = 4.32; ARC = 90°; THICKNESS = 0.1; E = $1.0 \times 10^7$; $\nu$ = 0.25; MESH = 6 x 1; LOADING: UNIT FORCES AT TIP.

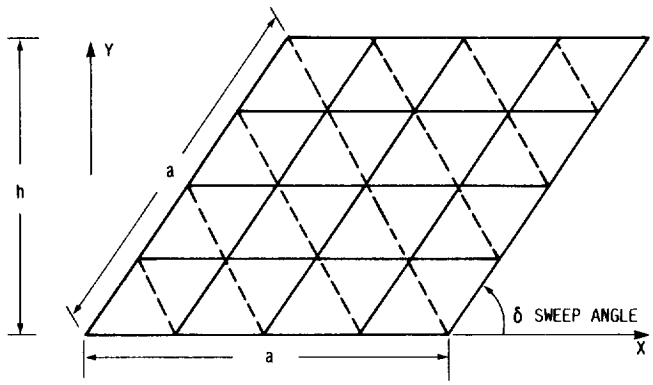


FIGURE 17. - MSGMESH TRIANGLE MESH IN MSC/NASTRAN.

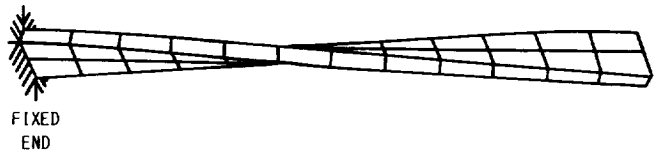


FIGURE 18. - TWISTED BEAM. LENGTH = 12.0; WIDTH = 1.1; DEPTH = 0.32; TWIST = $90^0$ (ROOT TO TIP); E = $29.0 \times 10^6$; $\nu$ = 0.22; MESH = 12 x 2; LOADING: UNIT FORCES AT TIP.

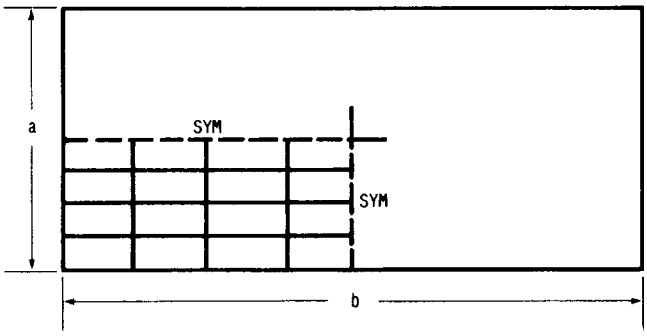


FIGURE 19. - RECTANGULAR PLATE. a = 2.0; b = 2.0 OR 10.0; THICKNESS = 0.0001 (PLATES); THICKNESS = 0.1 (SOLIDS); E = $1.7472 \times 10^7$; $\nu$ = 0.3; BOUNDARIES = SIMPLY SUPPORTED OR CLAMPED; MESH = N x N (ON 1/4 OF PLATE); LOADING: UNIFORM PRESSURE, q = $10^{-4}$ OR CENTRAL LOAD P = $4.0 \times 10^{-4}$.

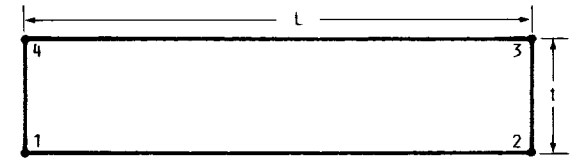


(A) ISOPARAMETRIC ELEMENT.

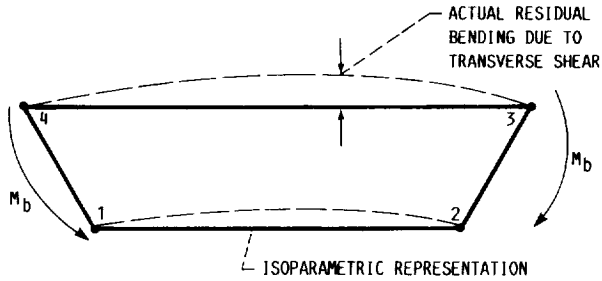


(B) PURE BENDING DEFORMATION.

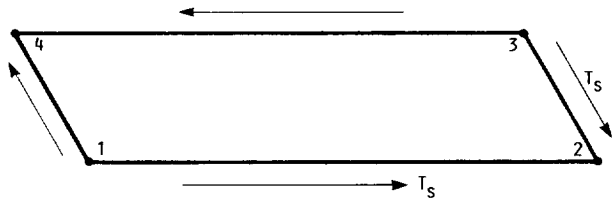


(C) PURE SHEAR DEFORMATION.

FIGURE 20. - DISTORTION MODES OF STANDARD ISOPARAMETRIC ELEMENTS.

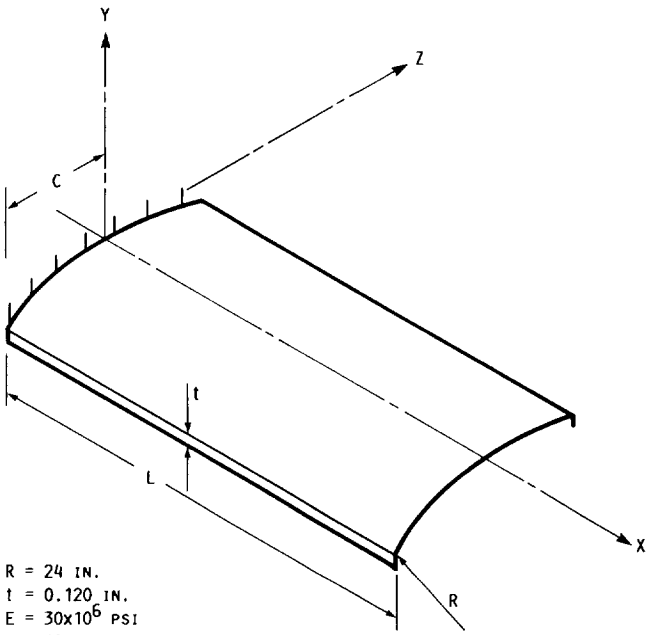


FIGURE 21. - VIBRATIONS OF A CAMBERED COMPRESSOR BLADE.

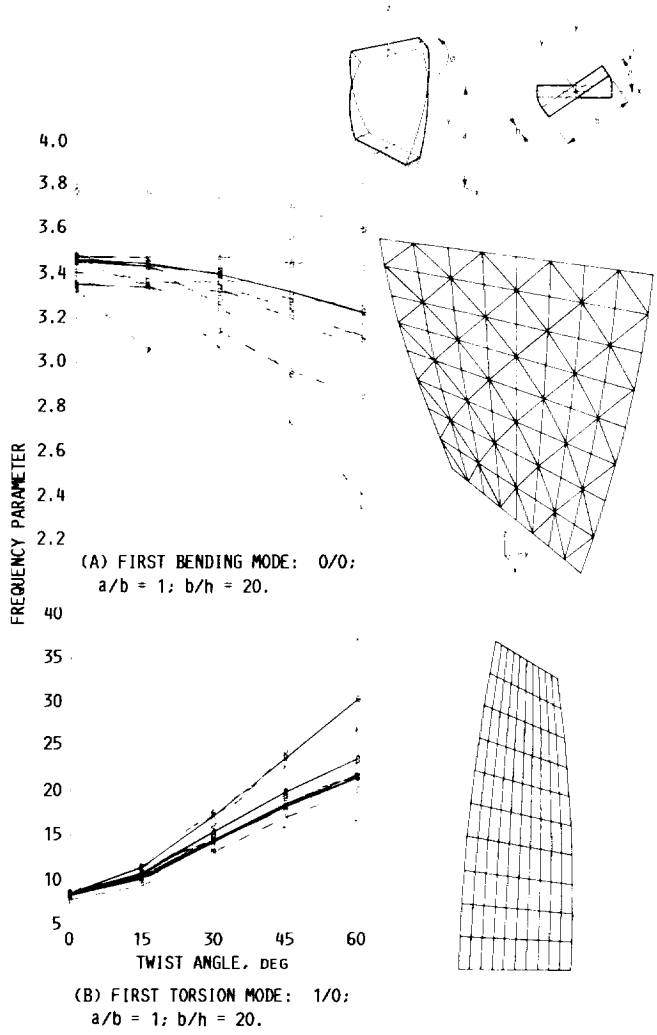


FIGURE 22. - DEPENDENCE OF FREQUENCY PARAMETER ON TWIST ANGLE.

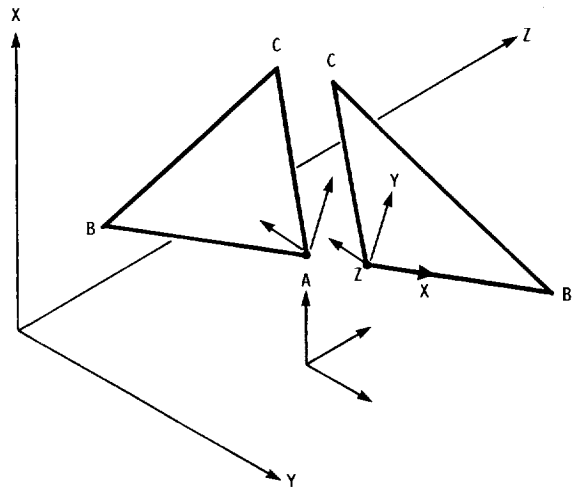


FIGURE 23. - CO-PLANAR ELEMENTS.

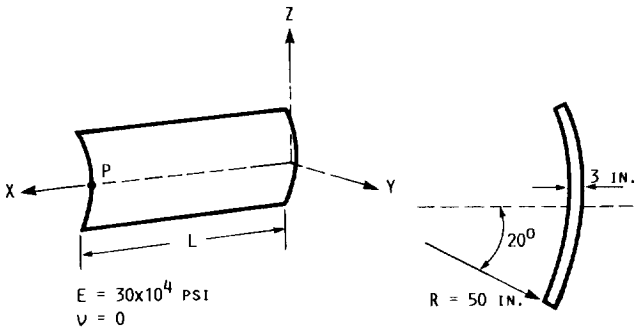


FIGURE 24. - EFFECT OF SIXTH DOF ON DEFLECTION OF CAMBERED BLADES.

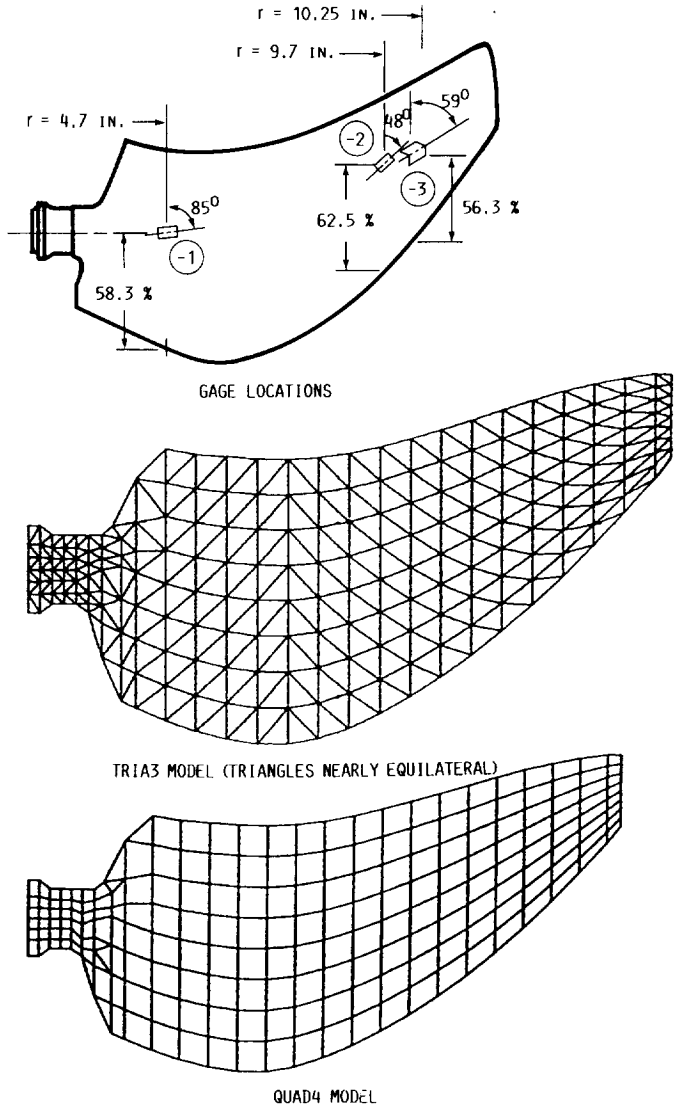


FIGURE 25. - SR-3C-3 PROPFAN BLADE - FINITE ELEMENT GRID.

NASA
National Aeronautics and Space Administration

# Report Documentation Page

| 1. Report No. | 2. Government Accession No. | 3. Recipient's Catalog No. |
|---|---|---|
| NASA TM-89906 | | |

| 4. Title and Subtitle | 5. Report Date |
|---|---|
| Finite Element Analysis of Flexible, Rotating Blades | July 1987 |
| | 6. Performing Organization Code: 535-03-01 |

| 7. Author(s) | 8. Performing Organization Report No. |
|---|---|
| Oliver G. McGee | E-3674 |
| | 10. Work Unit No. |

| 9. Performing Organization Name and Address | 11. Contract or Grant No. |
|---|---|
| National Aeronautics and Space Administration<br>Lewis Research Center<br>Cleveland, Ohio 44135 | |
| | 13. Type of Report and Period Covered: Technical Memorandum |

| 12. Sponsoring Agency Name and Address | 14. Sponsoring Agency Code |
|---|---|
| National Aeronautics and Space Administration<br>Washington, D.C. 20546 | |

15. Supplementary Notes

Summer Faculty Fellow. Present address: Ohio State University, Columbus, Ohio 43210.

16. Abstract

This report should be used as a reference guide when using the finite element method to approximate the static and dynamic behavior of flexible, rotating blades. Important parameters such as twist, sweep, camber, co-planar shell elements, centrifugal loads and inertia properties are studied. Comparisons are made between NASTRAN elements through published benchmark tests. The main purpose of this report is to summarize blade modeling strategies and to document capabilities and limitations (for flexible, rotating blades) of various NASTRAN elements.

| 17. Key Words (Suggested by Author(s)) | 18. Distribution Statement |
|---|---|
| Finite elements<br>NASTRAN<br>Blades | Unclassified - unlimited<br>STAR Category 39 |

| 19. Security Classif. (of this report) | 20. Security Classif. (of this page) | 21. No of pages | 22. Price* |
|---|---|---|---|
| Unclassified | Unclassified | 39 | A03 |

NASA FORM 1626 OCT 86

*For sale by the National Technical Information Service, Springfield, Virginia 22161